PHYSICAL REVIEW A **72**, 030702(R) (2005)

Simultaneous real-time tracking of wave packets evolving on two different potential curves in H_2^+ and D_2^+

A. S. Alnaser, B. Ulrich, X. M. Tong, I. V. Litvinyuk, C. M. Maharjan, P. Ranitovic, T. Osipov, R. Ali, S. Ghimire, Z. Chang, C. D. Lin, and C. L. Cocke

J. R. Macdonald Laboratory, Physics Department, Kansas State University, Manhattan, Kansas 66506-2601, USA

(Received 10 May 2005; published 29 September 2005)

We have used intense few-cycle laser pulses in a pump-probe arrangement to directly map, with high time resolution, the simultaneous evolution on two different potential curves of wave packets created when H_2 (D_2) molecules were ionized by a strong laser field. The experimental "snapshots" were obtained by measuring in coincidence the kinetic energy distribution of the proton (deuteron) pairs produced in the Coulomb explosion of the H_2^+ (D_2^+) molecular ions as a function of the time delay between the pump and the probe pulses. The time resolution was sufficient to reveal not only the evolution of the wave packet centroid but also the fundamentally wavelike features of the packets. A full quantum calculation of observed nuclear motion is in good agreement with the measured spectra.

DOI: 10.1103/PhysRevA.72.030702 PACS number(s): 32.80.Fb, 32.60.+i, 31.25.Jf

Visualization of the motion of the components of atomic and molecular systems on an atomic time scale allows us to form a mental picture of how dynamical physical processes that alter the internal state of atoms and molecules take place. Theoretically the time evolution of the wave function of any physical system is known, and in principle calculable, from the time-dependent Schrödinger equation (for nonrelativistic systems). The experimental observation of this evolution is more elusive, for reasons of both principle and practice. Due to the destructive nature of the "photography," a "molecular movie" must be made using a pump-probe approach: the system is prepared many times in an identical initial state, and a "snapshot" of the resulting system is taken after some delay. By taking many snapshots at different delay times the full dynamic evolution of the wave packet can be followed experimentally. The time scale on which this can be done has advanced rapidly from the early classic experiments [1–4], and 25 fs pulses are now routinely available. In this paper we take a further step down in time and work with 8 fs pulses. With the nonlinear nature of strong field tunneling ionization, we reach a time resolution of about one optical cycle of the laser pulse. This is a significant advance, since it allows the vibrational motion in even the simplest molecule, H_2^+, to be followed. We provide comprehensive multichannel coverage by tracking the wave packet on two different potential curves simultaneously. We are able to extract time-dependent features of the heavy particle motion that are clearly wave mechanical in nature and have no simple classical interpretation.

The schematic of the process we study is shown in Fig. 1. A short laser pump pulse removes one electron from a neutral H_2 (or D_2) molecule near the peak of the laser pulse, launching a wave packet onto the ground state potential curve of the H_2^+ system [5–8]. This wave packet has almost [9] the shape of the ground-state vibrational wave packet of the neutral hydrogen molecule, and is not stationary because the equilibrium distance, R, for H_2^+ (2.0 a.u.) is greater than that for H_2 (1.4 a.u.) and the curvature of the potential is less for the molecular ion. This packet now evolves and spreads in the $1s\sigma_g$ ground-state potential. In the presence of the tail of the laser pulse the $1s\sigma_g$ and $2p\sigma_u$ electronic curves are coupled, resulting in the generation of a second component of the wave packet propagating on the $2p\sigma_u$ potential curve. For the 800 nm radiation we use, this coupling becomes especially strong when the curves are separated by a single photon, which occurs near $R=4.6$ a.u. When parts of the

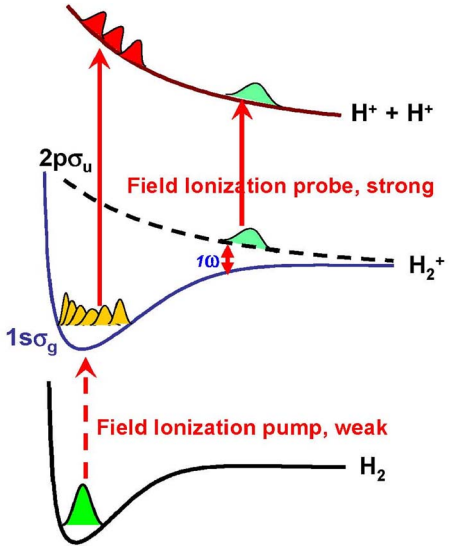

FIG. 1. (Color online) Schematic of pump-probe process in H_2. The weak pump pulse removes one electron from the neutral molecule near the peak of the laser pulse and launches the vibrational wave packet in the ground $1s\sigma_g$ state of H_2^+. The wave packet evolves outward and some part is coupled to the upper $2p\sigma_u$ curve in the tail of the laser field when the energy separation between the two curves is about one photon. The wave packet on the upper curve dissociates along the repulsive potential. The subsequent motion of the two wave packets can be probed experimentally with a strong probe pulse with adjustable delay. In the figure the ionization of the reflected lower wave packet is shown together with an outward evolving upper wave packet. The wave packet distributions are determined from the kinetic energy release of the protons.

packet reach this R, a non-negligible fraction of the wave packet may evolve from the $1s\sigma_g$ to the $2p\sigma_u$ curve, resulting ultimately in dissociation via the well-documented "bond-softening" process [10]. The remaining wave packet will oscillate in the $1s\sigma_g$ potential.

To put the above discussion on a quantitative basis, we have performed a quantum mechanical calculation to obtain the time evolution of the wave packet on the $1s\sigma_g$ and $2p\sigma_u$ potential surfaces in the laser field. The H_2 (D_2) molecule is ionized at the peak of the laser pulse, creating a wave packet moving initially on the $1s\sigma_g$ potential curve of H_2^+ (D_2^+). This wave packet is taken to be the ground-state vibrational wave function of the neutral hydrogen molecule. The subsequent motion of the wave packet is calculated by solving the following time-dependent Schrödinger equation

$$i\frac{\partial \chi_g(R,t)}{\partial t} = \left[-\frac{1}{2\mu}\frac{d^2}{dR^2} + V_g(R)\right]\chi_g(R,t) + V_{gu}(R)E(t)\chi_u(R,t),$$

$$i\frac{\partial \chi_u(R,t)}{\partial t} = \left[-\frac{1}{2\mu}\frac{d^2}{dR^2} + V_u(R)\right]\chi_u(R,t) + V_{gu}(R)E(t)\chi_g(R,t),$$

including only $1s\sigma_g$ and $2p\sigma_u$ potential curves. Here, χ_g and χ_u are the vibrational wave functions associated with the $1s\sigma_g$ and $2p\sigma_u$ states with potential curves V_g and V_u, respectively. The dipole coupling between the two electronic states is given by V_{gu}, μ is the reduced mass of the two nuclei, and $E(t)$ is the time-dependent laser field.

In Fig. 2 we show the long time behavior of the calculated time evolution of the density distributions of the two wave packets ($|\chi_g(R,t)|^2, |\chi_u(R,t)|^2$) associated with the $1s\sigma_g$ and $2p\sigma_u$ states of D_2^+ for D_2 ionized at the peak of an 8 fs laser pulse with peak intensity of 3×10^{14} W/cm^2. The equations were solved with the initial condition ($t=0$) that $\chi_g(R,t=0)$ is given by the ground vibrational wave function of D_2 and $\chi_u(R,t=0)=0$. For the wave packet on the upper $2p\sigma_u$ potential curve, the wave packet moves outward monotonically, except for a gradual spreading and some interference structure at long times. For the wave packet on the lower $1s\sigma_g$ curve, the behavior is oscillatory and quite complex.

How can these elementary theoretical predictions be observed experimentally? We sample the time evolution of the wave packet by using a strong probe pulse applied at a time τ after the pump pulse is over. This probe is strong enough that it can remove the remaining electron completely from the $2p\sigma_u$ potential curve, placing it on the H_2^{+2} Coulomb-exploding potential curve. The two protons then "Coulomb explode" with a kinetic energy release (KER), which is the sum of the Coulomb explosion energy plus a small contribution from the kinetic energy they have already accumulated by propagation along the $2p\sigma_u$ potential curve of the molecular ion. The strong probe laser also ionizes the electron from the $1s\sigma_g$ curve at a rate that increases as a function of internuclear separation R. We measure the KER and from it infer the internuclear distance at which this explosion occurred.

We have used a Ti:Sapphire laser with a 25 fs pulse width, 1-kHz repetition rate, 1.0 mJ pulse energy, 800 nm mean wavelength, compressed to 8 fs by passage through an argon-filled glass fiber [11]. The laser pulse is passed through a glass disk from which a central area of 5 mm has been cut and displaced along the direction of laser propagation. The pump pulse is formed from that part of the pulse that passes this disk, and the probe is formed from that which passes the remaining disk. The time delay is achieved by tilting the larger disk [12]. The focal point of both pulses is located inside a supersonic gas jet of molecular hydrogen (deuterium) with a local density near 10^6 atoms/cm^3. The resulting protons (deuterons) are projected onto the face of a channel plate detector located 5 cm away by a uniform transverse electric field of 20 V/cm. The position and time of arrival of each ion is used to reconstruct the *full* vector momenta with which they were emitted, on an event-by-event basis. Only coincident proton pairs corresponding to approximately zero momentum mother target molecules are accepted. Further experimental details are given in Refs. [13–15].

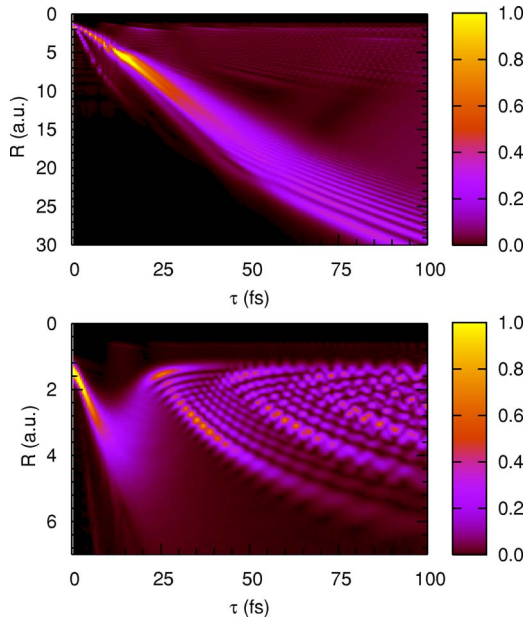

FIG. 2. (Color online) Calculated density plots of the vibrational wave packets associated with the $2p\sigma_u$ (upper panel) and $1s\sigma_g$ (lower panel) electronic states, as a function of time, generated by the ionization of a neutral deuterium molecule by a pulse of peak intensity 3×10^{14} W/cm^2 and pulse length 8 fs full width at half maximum (FWHM).

In Fig. 3 we show a density plot of the yield of coincident proton pairs, with the time delay on the horizontal axis and the KER on the vertical axis. The propagation of the wave packet on the $1s\sigma_g$ and $2p\sigma_u$ curves is readily apparent. As expected from the description above, the $1s\sigma_g$ packet oscillates back and forth in the $1s\sigma_g$ potential curve, giving rise to a KER centered near 8–9 eV with clear oscillatory behavior with a period near 15 fs. This KER is slightly lower than one might expect for a wave packet oscillating about a potential minimum of 2.0 a.u., since the ionization rate from this potential curve increases rapidly with internuclear distance [16]. The $2p\sigma_u$ packet is seen as a single descending trajectory giving rise to a KER decreasing monotonically from

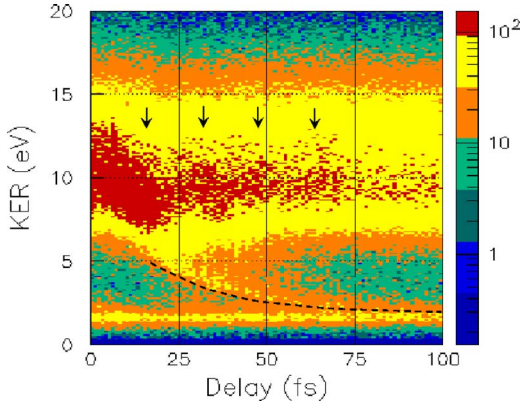

FIG. 3. (Color online) Density plot of the yield of coincident proton pairs from H_2. The vertical axis is the kinetic energy release of the protons and the horizontal axis is the delay time between pump and probe. The wave packet trapped in the $1s\sigma_g$ potential is seen centered near a KER of 8–9 eV and oscillates with a period near 15 fs. Recurrences are denoted by small vertical arrows. The packet on the dissociative $2p\sigma_u$ potential appears as a monotonically descending track evolving toward a KER of 2 eV at 100 fs. The classical trajectory expected for the $2p\sigma_u$ packet is shown as a black dashed line. The pump and probe are linearly polarized with peak intensities of 10^{14} W/cm^2 and intensity 10^{15} W/cm^2, respectively. The pulse length is 8 fs (FWHM).

about 6 eV at 20 fs to near 2 eV at 100 fs. We ask to what extent this trajectory can be accounted for classically. The black dashed line superimposed on the $2p\sigma_u$ curve of Fig. 3 shows the trajectory of a classical particle launched from rest, but with a delay, on the $2p\sigma_u$ curve. The delay was taken to be 7.8 fs, the time the particle would have taken to propagate on the $1s\sigma_g$ curve from 1.4 a.u. to the bond-softening crossing at 4.6 a.u., with enough initial kinetic energy to just reach this point. To avoid visual confusion on the figure, and because the identification of the dissociative wave packet becomes clear only beyond about 20 fs, only the part of this trajectory beyond this time is shown. The calculated KER is the sum of the KER from the Coulomb explosion and that accumulated on the dissociation potential. The classical trajectory is seen to track very near the experimental trajectory.

Can we observe the complex behavior of the $1s\sigma_g$ wave packet predicted in Fig. 3? Classically one would expect this packet to simply oscillate back and forth between the two turning points at $R=1.4$ and 3.5, and indeed evidence for such behavior was reported in [17]. The quantum calculation shows that the behavior of this packet is more interesting. After the first reflection from the outer turning point and within the next half period, the wave packet is very broad showing no noticeable localization within the potential well. At about one vibrational period, the wave packet "re-emerges" from the inner turning point and immediately thereafter produces one major peak moving outward with additional minor peaks. This pattern repeats itself at multiples of the vibrational period (about 21 fs for D_2^+). The additional minor peak structure results from the interference between the waves going on opposite directions, from components of different phase velocity.

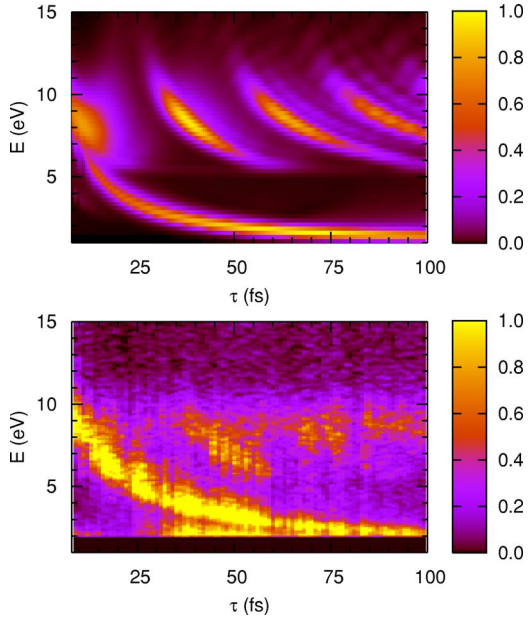

FIG. 4. (Color online) Lower panel: Similar to Fig. 3, but for a D_2 target and for pump and probe intensities of 3×10^{14} W/cm^2 and 9×10^{14} W/cm^2, respectively and a pulse length of 10 fs (FWHM). Upper panel: model calculation. The "outgoing waves" in the $1s\sigma_g$ potential curve, which are seen in the calculations of Fig. 2, appear in these spectra as descending stripes centered near a KER of 8 eV and recur with a period near 21 fs.

In the upper panel of Fig. 4 we show the corresponding theoretical KER spectrum assuming removal of the second electron by the delayed probe at a rate given by the exact static ionization rate [18]. The KER was calculated assuming a pure Coulomb explosion. The two-potential-curve nature seen in the data of Fig. 3 is clearly predicted, with an oscillatory packet in the $1s\sigma_g$ potential and a dissociative packet eventually following the $2p\sigma_u$ potential. The series of strong outgoing, but not incoming, waves seen in Fig. 2 for the $1s\sigma_g$ packet gives rise to a series of descending stripes on the $1s\sigma_g$ KER plot, with the outward motion of wave maxima much more prominent than any inward motion of the returning waves.

In order to search for these stripes experimentally, we performed the experiment with molecular deuterium, which produces a slightly more compact wave packet and a slower time evolution. The results are shown in the lower panel of Fig. 4. The sequence of outgoing waves predicted by the model is clearly observed in the data, showing that we are able to see in the experimental photographs not only the overall oscillatory motion of the wave packet but details of its dispersion and propagation that go beyond the classical description. We note that the theoretical calculation of the kinetic energy release is simply a reflection of the vibrational wave packet in the double ionization potential and does not include any kinetic energy accumulated by the wave packets in propagating along the potential curves. Thus the theoretical locus for the dissociative curve is somewhat lower than the experimental one.

In summary, we have shown that the simultaneous propagation of vibrational wave packets on different potential

curves can be tracked on a very short time scale in H_2^+ using a pump-probe arrangement. Along with the average motion along the potential curves, detailed structural features of the dispersing and propagating wave packets are revealed. If the pump pulses were replaced by custom-shaped pulses, quite technically feasible today, we believe one could use this approach to give quite specific time-dependent information about the shaping of vibrational wave packets. This might in turn prove extremely useful in being able to control the outcome of the dissociation process. Extensions to a broader range of chemical rearrangement processes could be possible [19].

This work was supported by Chemical Sciences, Geosciences and Biosciences Division, Office of Basic Energy Sciences, Office of Science, U. S. Department of Energy. The construction of the laser facility was partially supported by NSF MRI Grant No. Phys-0116070.

[1] A. H. Zewail, Nature (London) **348**, 225 (1990).
[2] A. H. Zewail, *Femtochemistry: Ultrafast Dynamics of the Chemical Bond*, World Scientific Series in 20th Century Chemistry (World Scientific, Singapore, 1994), Vol. 1, p. 2.
[3] H. Stapelfeldt, E. Constant, and P. B. Corkum, Phys. Rev. Lett. **74**, 3780 (1995).
[4] C. Petersen, E. Peronne, J. Thøgersen, H. Stapelfeldt, and M. Machholm, Phys. Rev. A **70**, 033404 (2004).
[5] A. S. Alnaser, T. Osipov, E. P. Benis, A. Wech, B. Shan, C. L. Cocke, X. M. Tong, and C. D. Lin, Phys. Rev. Lett. **91**, 163002 (2003).
[6] A. S. Alnaser, X. M. Tong, T. Osipov, S. Voss, C. M. Maharjan, P. Ranitovic, B. Ulrich, B. Shan, Z. Chang, C. D. Lin, and C. L. Cocke, Phys. Rev. Lett. **93**, 183202 (2004).
[7] H. Niikura, F. Legare, R. Hasbani, M. Y. Ivanov, D. M. Villeneuve, and P. B. Corkum, Nature (London) **421**, 826 (2003).
[8] X. M. Tong, Z. X. Zhao, and C. D. Lin, Phys. Rev. A **68**, 043412 (2003).
[9] X. Urbain, B. Fabre, E. M. Staicu-Casagrande, N. de Ruette, V. M. Andrianarijaona, J. Jureta, J. H. Posthumus, A. Saenz, E. Baldit, and C. Cornaggia, Phys. Rev. Lett. **92**, 163004 (2004).
[10] P. H. Bucksbaum, A. Zavriyev, H. G. Muller, and D. W. Schumacher, Phys. Rev. Lett. **64**, 1883 (1990).
[11] M. Nisoli, S. DeSilvestri, O. Svelto, R. Szipocs, K. Ferencz, C. Spielmann, S. Sartania, and F. Krausz, Opt. Lett. **22**, 522 (1997).
[12] P. M. Paul, E. S. Toma, P. Breger, G. Mullot, F. Auge, P. Balcou, H. G. Muller, and P. Agostini, Science **292**, 1689 (2001).
[13] R. Doerner *et al.*, Phys. Rep. **330**, 95 (2000).
[14] J. Ullrich, R. Moshammer, R. Dorner, O. Jagutzki, V. Mergel, H. Schmidt-Bocking, and L. Spielberger, J. Phys. B **30**, 2917 (1997).
[15] S. Voss, A. S. Alnaser, X. M. Tong, C. Maharjan, P. Ranitovic, B. Ulrich, B. Shan, Z. Chang, C. D. Lin, and C. L. Cocke, J. Phys. B **37**, 4239 (2004).
[16] A. Bandrauk, Comments At. Mol. Phys. **1**(3), D, 97 (1999).
[17] F. Legare, K. F. Lee, P. W. Dooley, D. M. Villeneuve, P. B. Corkum, A. D. Bandrauk, and I. V. Litvinyuk, Proceedings of the International Conference on Ultrafast Phenomena, Niigata, Japan, 2004 (unpublished).
[18] X. M. Tong, Z. X. Zhao, and C. D. Lin, Phys. Rev. A **66**, 033402 (2002).
[19] F. Legaré, K. F. Lee, I. V. Litvinyuk, P. W. Dooley, S. S. Wesolowski, P. R. Bunker, P. Dombi, F. Krausz, A. D. Bandrauk, D. M. Villeneuve, and P. B. Corkum, Phys. Rev. A **71**, 013415 (2005).